Engineered Science
DOI: https://dx.doi.org/10.30919/es1030

Application of Finite Element Method for Solving Seismoacoustic Modeling Problems in Poroelastic Composite Media

M. Nurtas,[1, 2,*] F. Tokmukhamedova,[1,*] A. Ydyrys,[1,*] Zh. Zhantaev,[1] S. Nurakynov,[2] B. Iskakov,[2] A. Altaibek[1, 2] and B. Matkerim[3]

Abstract

The present study is devoted to solving the problem of seismic and acoustic wave propagation in the porous media for composite domains. For simplicity, simple geometry was selected, where domain Ω in consideration consists of three different domains $\Omega_k, k = 1, 2, 3$ with different physical and geometrical properties. The wave propagation in the solid skeleton Ω_s of Ω is governed by the Lame's equations. The fluid dynamics in the liquid domain $\Omega_f = \cup_{k=1}^{3} \Omega_{f,k}$ is governed by the Stokes equations. To model the geometry, we postulate that there are two small parameters: the dimensionless size of pores ε and the dimensionless size of fractures δ and $\varepsilon \leq \delta$, where $\varepsilon = \frac{l}{L}$ is the dimensionless pore size, l is the average size of pores. Domains $\Omega_{f,1}$ and $\Omega_{f,3}$ have the ε-periodic structure and the domain $\Omega_{f,2}$ has the δ-periodic structure with $\varepsilon = \delta^r, 0 < r < 1$. At the common boundaries of the 'liquid-solid' area, the usual continuity condition of continuum mechanics holds. The main goal of the study is the numerical implementations using finite element method (FEM) for the analysis of wave propagation in Ω. The impact of the study on the composites field offers valuable insights into materials' behavior under dynamic loading conditions, improving the composite structures across industries.

Keywords: Stokes and Lame equations; Wave propagation; Fractured porous media; Numerical simulation; Finite element method.
Received: 09 October 2023; Revised: 14 October 2023; Accepted: 16 October 2023.
Article type: Research article.

1. Introduction

Poroelastic composite media are intricate material structures characterized by a blend of solid matrices and fluid-filled pores. They are commonly encountered in geological formations and various engineering applications. Within the realm of seismic acoustics, these media serve as vital tools for comprehending wave propagation and interactions.

Seismic and acoustic wave propagation[1,2] through porous media[2] holds immense significance due to its widespread applications and the insights it provides into subsurface characteristics. Understanding these wave behaviors in porous media is pivotal for various scientific, industrial, and environmental fields.

[1] *Department of Mathematical and Computer Modelling, International Information Technology University, 34/1 Manas Street, 050040, Almaty, Kazakhstan.*
[2] *Institute of Ionosphere, 117 Gardening community IONOSPHERE, 050020, Almaty, Kazakhstan.*
[3] *Department of Computer Science, Faculty of Mechanics and Mathematics, Al-Farabi Kazakh National University, 71 Al-Farabi Avenue, 050040, Almaty, Kazakhstan.*
**Email:* m.nurtas@iitu.edu.kz, maratnurtas@gmail.com (M. Nurtas); f.tokmukhamedova@iitu.edu.kz (F. Tokmukhamedova); a.ydyrys@iitu.edu.kz (A. Ydyrys)

Hydrocarbon exploration

Seismic waves[3] are fundamental in oil and gas exploration, aiding in locating hydrocarbon reservoirs beneath the Earth's surface. By studying how these waves travel through porous rock formations, geophysicists can estimate critical properties such as porosity, permeability, and fluid saturation. Example: Seismic waves encountering an oil reservoir experience distinct speed and amplitude changes due to the contrasting properties of oil-filled pores compared to the surrounding rock. This change serves as a clear indicator of potential hydrocarbon reservoirs.

Geotechnical engineering

Seismic wave analysis[4,5] in porous media is essential for assessing the stability and safety of structures. Engineers utilize this knowledge to analyze wave behavior in various types of soils and substrates, crucial for designing foundations resilient to seismic activity.

Example: Before constructing a building, engineers study how seismic waves will interact with the building's foundation. Understanding this interaction helps design structures that can withstand potential seismic events.

Environmental studies

Seismic wave propagation is a valuable tool for studying subsurface layers and aquifers, aiding in assessing groundwater resources, soil composition, and potential environmental contamination. Example: Researchers employ seismic waves to assess the porosity of underground aquifers, a critical parameter for sustainable water management and environmental conservation.

The theoretical understanding of seismic and acoustic wave propagation in porous media is rooted in the principles of wave physics, fluid dynamics, and solid mechanics. It involves complex mathematical models, including Biot's theory[1-3] which describes wave behavior in fluid-saturated porous media, considering the interactions between solid matrix, fluid, and the pores. Over the years, researchers have refined these theoretical models, incorporating geological complexities and fluid dynamics to create more accurate representations of real-world porous media. Advanced numerical simulations and experimental studies have further enriched our understanding, enabling us to make precise predictions and optimize applications in various domains. This background of theoretical studies forms the foundation for leveraging seismic and acoustic wave propagation to unravel subsurface mysteries and enhance diverse technological endeavors.

Let the dimensionless variables $\Omega = \{x = (x_1, x_2, x_3) \in R^3 : x_1 + x_2 < \frac{1}{2}, 0 < x_3 < H\} = \Omega_f \cup S \cup \Omega_s$. Poroelastic composite media[1-3] is the parallelepiped consisting of three subdomains: $\Omega_1 = \left\{\boldsymbol{x} = (x_1, x_2, x_3) \in R^3 : x_1 + x_2 < \frac{1}{2}, x_1 + x_2 < \frac{1}{2}, 0 = H_0 < x_3 < H_1\right\}$, $\Omega_2 \left\{\boldsymbol{x} = (x_1, x_2, x_3) \in R^3 : x_1 + x_2 < \frac{1}{2}, x_1 + x_2 < \frac{1}{2}, H_1 < x_3 < H_2\right\}$ and $\Omega_3 = \left\{\boldsymbol{x} = (x_1, x_2, x_3) \in R^3 : x_1 + x_2 < \frac{1}{2}, x_1 + x_2 < \frac{1}{2}, H_2 < x_3 < H_3 = H\right\}$. Ω_1 and Ω_3 are supposed to be the poroelastic composite media: $\Omega_k = \Omega^\varepsilon_{f,k} \cup S^\varepsilon_k \cup \Omega^\varepsilon_s, k = 1,3$ and Ω_2 is a fractured porous medium : $\Omega_2 = \Omega^\delta_{2,f} \cup S^\delta_2 \cup \Omega^\delta_{2,s}, S^\varepsilon = S^\varepsilon_1 \cup S^\delta_2 \cup S^\varepsilon_3$.

For our future numerical experiments, ' H ' represents the depth of the poroelastic composite media in the half-space, measured in meters. Accordingly, 'H_0' represents the surface of the composite media, respectively 'H_1,' 'H_2,' and 'H_3' marks the boundaries separating the inner layers of the composite media due to their distinct physical properties.

Composite material has a macroscopic shape and a microstructure. The ratio between the size of the microstructure and the size of the material is ε. In order to make the purpose clear, we first consider the simplest - but rich enough example we know. (The explanation that follows does not aim to be mathematically rigorous. It clearly appeals to intuition and to non-rigorous vocabulary.) Imagine that we want to get the pressure field within a composite material which is in poroelastic composite media, knowing the reflection waves on its boundaries. Symbolically, as represented in Fig. 1 (in a bi-dimensional setting), the composite material has a macroscopic shape at a macroscopic size. Within it, heterogeneities are more or less periodically distributed with a periodicity - or a characteristic size - which is ε times smaller than its macroscopic size, where ε is a small parameter.

In the solid skeleton Ω^ε_S, the displacements $\boldsymbol{w}^\varepsilon$ and the pressure p^ε_S of the solid skeleton satisfy the Lame equations:[4,5]

$$\frac{\partial^2 \boldsymbol{w}^\varepsilon}{\partial t^2} = \nabla \cdot P^\varepsilon_S, P^\varepsilon_S = \nu(\boldsymbol{x}) D(x, \boldsymbol{w}^\varepsilon) - p^\varepsilon_S I \quad (1)$$

In the liquid domain Ω^ε_f, the velocity $v^\varepsilon = \frac{\partial w^\varepsilon}{\partial t}$ and the pressure p^ε_f satisfy the Stokes equations:

$$\frac{\partial \boldsymbol{v}^\varepsilon}{\partial t} = \nabla \cdot \mathbb{P}^\varepsilon_f,\ \mathbb{P}^\varepsilon_f = \lambda(\boldsymbol{x}) \mathbb{D}(x, \boldsymbol{v}^\varepsilon) - p^\varepsilon_f \mathbb{I}. \quad (2)$$

The differential equations in composite media Ω were completed with the state equation as:

$$p^\varepsilon = c^2(x) \varrho^\varepsilon. \quad (3)$$

Finally, at the common boundary, S^ε holds true for the continuity condition of classical Newtonian continuum mechanics:[6]

$$\boldsymbol{w}^\varepsilon(\boldsymbol{x}_0 + 0, t) = \boldsymbol{w}^\varepsilon(\boldsymbol{x}_0 - 0, t),$$
$$\mathbb{P}^\varepsilon_f(\boldsymbol{x}_0 + 0, t) < \boldsymbol{n} >= \mathbb{P}^\varepsilon_S(\boldsymbol{x}_0 - 0, t) < \boldsymbol{n} >, \quad (4)$$

The boundary conditions can be defined as:

$$\mathbb{P}^\varepsilon < \boldsymbol{e}_3 >= -p_H(\boldsymbol{x}) \boldsymbol{e}_3,\ x_3 = 0, \quad (5)$$
$$\mathbb{P}^\varepsilon < \boldsymbol{e}_3 >= -p_H(\boldsymbol{x}) \boldsymbol{e}_3,\ x_3 = H \quad (6)$$

and initial conditions can be described as:

$$\boldsymbol{w}^\varepsilon(x, 0) = \boldsymbol{w}^\varepsilon_0(\boldsymbol{x}) \quad (7)$$
$$p^\varepsilon(\boldsymbol{x}, 0) = p^\varepsilon_0(\boldsymbol{x}). \quad (8)$$

where $\mathbb{P}^\varepsilon < \boldsymbol{e}_3 >= -p_H(\boldsymbol{x}) \boldsymbol{e}_3,\ x_3 = 0,\ const > 0$ is the viscosity of the liquid, $c(\boldsymbol{x}) = \chi^\varepsilon c_f + (1 - \chi^\varepsilon) \sum_{k=1}^{3} c_{s,k} \xi_k, \xi_k(x) = 1$ for $\boldsymbol{x} \in \Omega^\varepsilon_{s,k}$ and are equal zero outside of $\Omega^\varepsilon_{s,k}$, $c_{s,k} = const > 0$ are the speed of sound in $\Omega^\varepsilon_{s,k}$,

$$\boldsymbol{v}^\varepsilon(\boldsymbol{x}_0 + 0, t) = \lim_{\boldsymbol{x} \to \to \boldsymbol{x}_0} \boldsymbol{v}^\varepsilon(\boldsymbol{x}, t), \boldsymbol{x} \in \Omega^\varepsilon_f, \boldsymbol{x}_0 \in S^\varepsilon$$
$$\boldsymbol{v}^\varepsilon(\boldsymbol{x}_0 - 0, t) = \lim_{\boldsymbol{x} \to \boldsymbol{x}_0} \boldsymbol{v}^\varepsilon(\boldsymbol{x}, t), \boldsymbol{x} \in \Omega^\varepsilon_s,\ \boldsymbol{x}_0 \in S^\varepsilon$$

and $\boldsymbol{n}$ is the unit normal vector to the boundary S^ε.

$$\mathbb{P}^\varepsilon = \chi^\varepsilon \mathbb{P}^\varepsilon_f + (1 - \chi^\varepsilon) \mathbb{P}^\varepsilon_s \quad (9)$$

In this study, the microscopic model of the physical process in consideration was derived. The formal method of three scale decomposition[7,8] was used to get the corresponding macroscopic model.

Transforming seismoacoustic equations from the microscopic to macroscopic form in poroelastic composite media simplifies complex descriptions of wave interactions. This transition facilitates practical analysis and extends applications in geophysics and engineering. It empowers researchers and practitioners to effectively predict wave behavior within poroelastic composites.

2. Auxiliary statements

2.1 Matrices and differential operators

$\mathbb{A}, \mathbb{B}$ and $\mathbb{C}$ denote tensors (linear transformations $\mathbb{R}^3 \to \mathbb{R}^3$). $(A), (B)$ and (C) denote the corresponding matrices in some Cartesian coordinate system.

The product $\mathbb{C} = \mathbb{A} \cdot \mathbb{B}$ is a transformation $\mathbb{R}^3 \to \mathbb{R}^3$, where, $\mathbb{C} < \boldsymbol{x} >= \mathbb{A} < (\mathbb{B} < \boldsymbol{x} >) >$.

$\mathbb{I}$ is a unit tensor: $\mathbb{I} \cdot \mathbb{A} = \mathbb{A} \cdot \mathbb{I} = \mathbb{A}$ for any tensor $\mathbb{A}$.

Let $\mathbb{A}$ be tensor. As $\mathbb{A}^*$ denote the tensor $\mathbb{B}$, such that $(\mathbb{A} < \boldsymbol{x} >, \boldsymbol{y}) = (\boldsymbol{x}, \mathbb{B} < \boldsymbol{y} >)$ for all $(\equiv \forall) \boldsymbol{x}, \boldsymbol{y} \in \mathbb{R}^3$.

$\boldsymbol{a} \otimes \boldsymbol{b}$ we denote the diad(second-order tensor),[9] which is defined for any two vectors $\boldsymbol{a}$ and $\boldsymbol{b}$ so that for any vector $\boldsymbol{c}$ the action of the tensor $\boldsymbol{a} \otimes \boldsymbol{b}$ to the vector $\boldsymbol{c}$ is given by the formula $(a \otimes b) \cdot c = a(b \cdot c)$.

For second-order tensors $\mathbb{A}$ and $\mathbb{B}$ as the form $\mathbb{A} : \mathbb{B}$ we denote the number transformation $tr\,(\mathbb{A} \cdot \mathbb{B}^*)$ as $tr\,(\mathbb{A} \cdot \mathbb{B}^*) = \sum_{i,j=1}^{3} a_{ij} b_{ji}$.

Let $\{\boldsymbol{e}^1, \boldsymbol{e}^2, \boldsymbol{e}^3\}$ be the standard Cartesian basis in $\mathbb{R}^3$. Then we put $\mathbb{J}^{ij} = \frac{1}{2}\left(\boldsymbol{e}^i \otimes \boldsymbol{e}^j + \boldsymbol{e}^j \otimes \boldsymbol{e}^i\right)$.

Use for any second-order tensors $\mathbb{A}, \mathbb{B}$, $\mathbb{C}\mathbb{A} \otimes \mathbb{B}$ we can write is a fourth-order tensor[9] form: $(\mathbb{A} \otimes \mathbb{B}) : \mathbb{C} = \mathbb{A}(\mathbb{B} : \mathbb{C})$. Operators $\nabla, \nabla', \nabla \cdot$ without indices mean differentiation with respect to the variable $\boldsymbol{x}$:

$$\nabla u = \left(\frac{\partial u}{\partial x_1}, \frac{\partial u}{\partial x_2}, \frac{\partial u}{\partial x_3}\right), \nabla' u = \left(\frac{\partial u}{\partial x_1}, \frac{\partial u}{\partial x_2}\right), \nabla \cdot \boldsymbol{v} = \sum_{k=1}^{3} \frac{\partial v_k}{\partial x_k},$$

$\triangle\, u = \nabla \cdot (\nabla u), \triangle\, \boldsymbol{u} = (\triangle\, u_1, \triangle\, u_2, \triangle\, u_3)$,

$\nabla' \cdot \boldsymbol{u}' = \frac{\partial u_1}{\partial x_1} + \frac{\partial u_2}{\partial x_2}, \triangle'\, u = \nabla' \cdot (\nabla' u) = \sum_{k=1}^{2} \frac{\partial^2 u_k}{\partial x_k^2}$.

$$\nabla \cdot \left(\frac{\partial \boldsymbol{v}}{\partial \boldsymbol{x}}\right) = \triangle\, \boldsymbol{v}, \nabla \cdot (\mathbb{D}(x, \boldsymbol{v})) = \frac{1}{2}\nabla(\nabla \cdot \boldsymbol{v}) + \frac{1}{2}\triangle\, \boldsymbol{v} \quad (10)$$

$$\nabla \cdot \left(\frac{\partial \boldsymbol{v}^*}{\partial \boldsymbol{x}}\right) = \nabla(\nabla \cdot \boldsymbol{v}) \quad (11)$$

$$\nabla \cdot \left(\frac{\partial \boldsymbol{v}}{\partial \boldsymbol{x}}\right) = \triangle\, \boldsymbol{v} \quad (12)$$

$$\nabla \cdot (\mathbb{D}(x, \boldsymbol{v})) = \frac{1}{2}\nabla(\nabla \cdot \boldsymbol{v}) + \frac{1}{2}\triangle\, \boldsymbol{v} \quad (13)$$

Let $\boldsymbol{u} = (u_1, u_2, u_3)$ and $D(x, \boldsymbol{u}) = \frac{1}{2}(\nabla_x \boldsymbol{u} + (\nabla_x \boldsymbol{u})^*)$. Then the second-order tensor

$$\mathbb{D}(x, \boldsymbol{u}) = \begin{pmatrix} d_{11} & d_{12} & d_{13} \\ d_{21} & d_{22} & d_{23} \\ d_{31} & d_{32} & d_{33} \end{pmatrix},$$

where $d_{ik} = \frac{1}{2}\left(\frac{\partial u_m}{\partial x_k} + \frac{\partial u_k}{\partial x_m}\right), m, k = 1,2,3 \ldots$, is called the symmetric gradient of the vector $\boldsymbol{u}$.

2.2 Integration by parts (Green's identity)

Takes place the following formulae:[9]

$$\int_{\Omega} \nabla \cdot \boldsymbol{u} dx = \int_{\partial\Omega} \boldsymbol{u} \cdot \boldsymbol{n} d\sigma$$

for any smooth function $\boldsymbol{u}$.

In Eq. (1), $\partial\Omega$ is the $\mathbb{C}^1$-boundary of the domain Ω, and n is the outward to Ω unit normal to $\partial\Omega$.

2.3 Equivalent formulation of the problem (Eq. 1) - (Eq. 6) as a system of integral identities

To reformulate the problem Eqs. (1-6) as a system of integral identities, we first consider new stress tensor,[10-14]

$$\widehat{\mathbb{P}}^\varepsilon = \mathbb{P}^\varepsilon - p_H(\boldsymbol{x})\mathbb{I},\ p_H(\boldsymbol{x}) = \frac{1}{H}(p_a(H - x_3) + p_* x_3) \quad (14)$$

and rewrite Eqs. (1-2) and boundary conditionsEqs. (4-6) as:

$$\frac{\partial^2 \boldsymbol{w}^\varepsilon}{\partial t^2} = \nabla \cdot \widehat{\mathbb{P}}_s^\varepsilon + \nabla p_H,\ \boldsymbol{x} \in \Omega_s^\varepsilon,\ t > 0, \quad (15)$$

$$\frac{\partial v^\varepsilon}{\partial t} = \nabla \cdot P_f, x \in \Omega_s^\varepsilon, t > 0, \quad (16)$$

$$\boldsymbol{w}^\varepsilon(\boldsymbol{x}_0 + 0, t) = \boldsymbol{w}^\varepsilon(\boldsymbol{x}_0 - 0, t),$$
$$\mathbb{P}_s^\varepsilon(\boldsymbol{x}_0 + 0, t) < \boldsymbol{n} >= \mathbb{P}_s^\varepsilon(\boldsymbol{x}_0 - 0, t) < \boldsymbol{n} >,$$
$$\mathbb{P}_f^\varepsilon(\boldsymbol{x}_0 + 0, t) < \boldsymbol{n} >= \mathbb{P}_f^\varepsilon(\boldsymbol{x}_0 - 0, t) < \boldsymbol{n} > \quad (17)$$

here, p_a is the atmospheric pressure, p_* is the given pressure at the level $x_3 = H$.

multiply the Eqs. (15-16) by some smooth vector-function $\boldsymbol{\varphi}$, integrate over each domain[15,16] Ω_k, $k = 1, 2, 3$ and then summarize the result, taking into account boundary conditions Eqs. (1-6):[17]

$$0 = \int_0^T \int_\Omega \widehat{\mathbb{P}}^\varepsilon : \mathbb{D}(x, \boldsymbol{\varphi}) dx d dt$$
$$= \int_0^T \int_\Omega \left(\chi^\varepsilon \widehat{\mathbb{P}}_f^\varepsilon + (1 - \chi^\varepsilon)\widehat{\mathbb{P}}_s^\varepsilon\right) : \mathbb{D}(x, \boldsymbol{\varphi}) dx dt$$
$$= \int_0^T \int_\Omega \left(\chi^\varepsilon(\nu\mathbb{D}(x, \boldsymbol{v}^\varepsilon) + \gamma\nabla \cdot \boldsymbol{v}^\varepsilon \mathbb{I} + (1 - \chi^\varepsilon)\mathbb{D}(x, \boldsymbol{w}^\varepsilon)\right):$$
$$\mathbb{D}(x, \boldsymbol{\varphi}) dx dt. \quad (18)$$

Further the focus of this article is centered solely on model (Eq. (18)), in which coefficients of Eqs. (1-9) depend continuously on the small parameter ε, $\mathbb{P}^\varepsilon = \chi^\varepsilon \mathbb{P}_f^\varepsilon + (1 - \chi^\varepsilon)\mathbb{P}_s^\varepsilon$ and $\{\boldsymbol{w}^\varepsilon, p^\varepsilon, v^\varepsilon, \varrho^\varepsilon\}$ is a corresponding generalized solution. We aim to find out the limiting regimes of the model and in passing to the limit, as ε goes to 0.

2.4 Numerical representation

The computation of partial differential equations on heterogeneous area[18] sometimes requires flexible methods and the finite element method is among them.[19] The method is practically convenient since the discretization of any shape is possible. Therefore, the idea of this method[20] is very beneficial because there is approximately no such thing with perfect shape in nature. Also, the ability to discretize boundary conditions[21,22] with derivatives is very advantageous. In addition, unstructured computational domain can give us more narrow answer for the particular area of interest, without any complication.

The main idea of the finite element method[23] is that the particular solution of the differential equation is considered as partitions called elements. Moreover, the result is dicretized on these partitions applying test function, which can be low-order polynomials. The second-order linear differential equation with constant coefficients is considered.[24,25]

The schematic representation of the given domain is shown in Fig. 1. In our experimental situation, we observe the propagation and reflection of a wave propagating from the upper boundary zone x=0 in media with different physical properties.[26] This experiment, in turn, is a test of how well our mathematical model works in real situations.

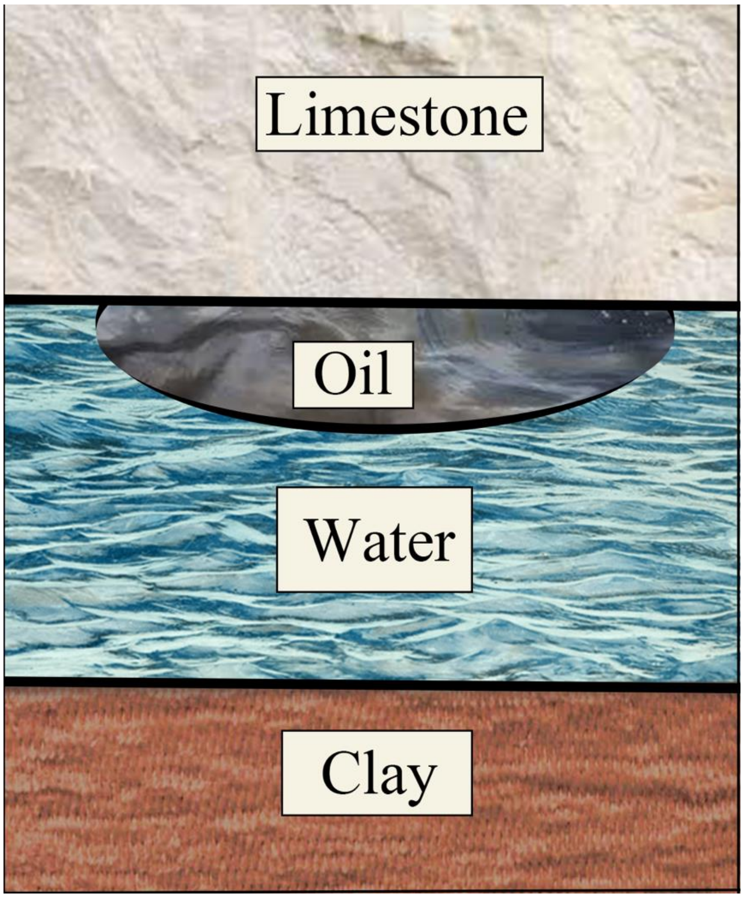

Fig. 1 Schematic representation of the poroelastic composite media with different physical domains.

3. Results and discussion

The purpose of this work is to obtain numerical solution of the poroelastic wave equation[17-19] in composite media[10] using the finite element method.[11] Firstly, the given model was theoretically covered and numerical solution's implementation was constructed.[10,11] The poroelastic wave equation was determined by Second Law of Newton.[8] A unique function was designed in order to provide significant altercations of physical properties of every material in each subarea with the characteristic function, which can only be either one or zero.[27] The seismoacoustic wave equation conversion linking the change in properties movement on every medium (density and speed of sound) results in the equation with specific changes in pressure with two variables: in space and by time.

The mathematical model was then constructed. Using the integral identity (Eq. (18)) to Eqs. (15-17) in Section 2.3, we have transferred the original model from the microscopic level to the macroscopic form. Now all our equations are independent of ε and the conditions Eqs. (5-6) and Eqs. (7-8) are satisfied.

$$\frac{\partial^2 \boldsymbol{w}}{\partial t^2} - \nabla \cdot \mathbb{P} = 0,\ \boldsymbol{x} \in \Omega_l,\ t > 0, \tag{19}$$

$$\mathbb{P} = \gamma_l \mathbb{D}(x, \boldsymbol{w}) - P\mathbb{I},\ l = 1, 2, 3 \tag{20}$$

when we take on the values $l = 1, 2$ and 3, it designates the sequence number of each medium in our experiment. This implies that the generalized equations (19) and (20) can be treated as three separate equations, each tailored to the specific physical properties of its corresponding medium. The solution of the system of differential Eqs. (19-20) constructed by fixing the boundaries of these media and imposing the continuity condition between them, despite the variety of physical properties of the different media under consideration, yields the solution of this model presented in Fig. 1. The fluid in the pores of a solid domain is moving and this condition is excluded.[14,17]

Given the graph of the numerical solution given in Fig. 2, the reflection of acoustic wave in every domain is shown. This means that a serious change in pressure occurred. In addition, the color visualization in every domain states the difference between physical parameters in each layer. These reflected waves play a very important role in real practical situations. The reflected waves can be obtained by receiving sensors, and by looking at the frequency of the seismic waves, we can find out what kind of medium they come from. It is clear that this is very useful information for seismic research.

In our previous studies, we examined the analytical solution for the specific case of[10] and the numerical solution for the particular case of[11] among the general models. However, the finite difference method was employed in the numerical model, and the outcome did not align with our expectations. In this current model, the result achieved through the finite element method is stable and closely approximates the practical value.

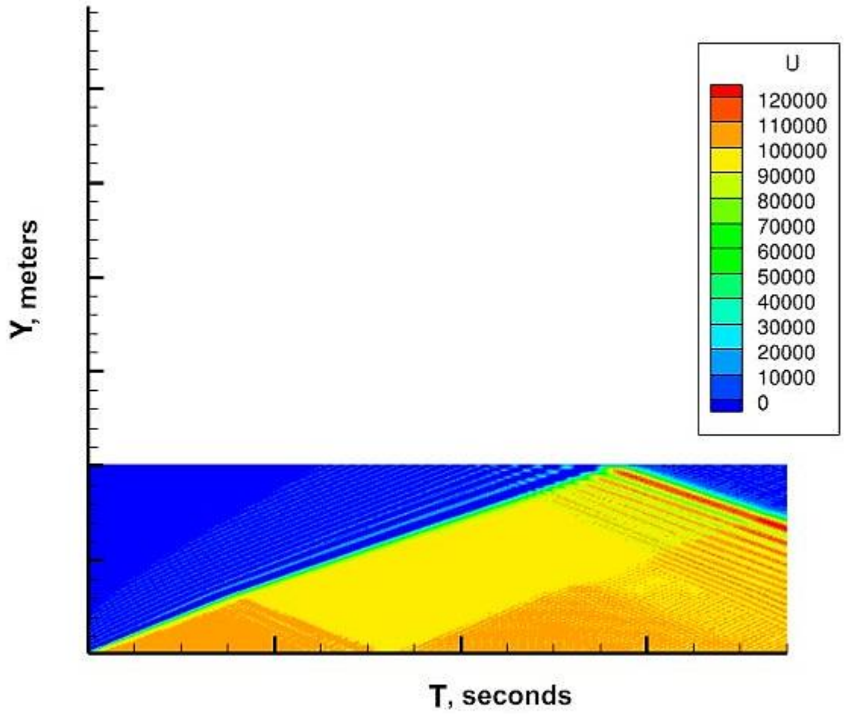

Fig. 2 Numerical representation by using finite elements (T - time (s), Y - depth (m)), maximal depth is $3000\ m.$, time - $75\ s.$).

The reflection on the wall of the region is distinct. The method made it possible to see a more preserved difference from the initial wave. This work provides a possible way to consider two- and three-dimensional space for acoustic wave equation with next aim to construct the neural networks and the deep learning methods for solving inverse problem.

4. Conclusion

A mathematical model describing the propagation of seismic and acoustic waves in a complex inhomogeneous media has been created. Considering this media as a poroelastic media due to the physical properties, the media can be divided into three different regions. The mathematical models related to each region were created. Due to the complexity of the obtained equations and the difficulty of microscopic nature, a new mathematical model was obtained using integral identities in order to transform them into macroscopic form. Finally, a numerical experiment was carried out based on the obtained equation. The above results of modeling seismoacoustic propagation in poroelastic media, representing the medium parameters as reflected data, are an important preliminary step before the direct numerical and machine-learning solutions of the inverse problem. The finite element method for solving seismoacoustic modeling problems in poroelastic media was applied. As shown in the experiment, the result obtained by applying the finite element method to a given mathematical model in subsurface layers consisting of three media with different physical properties is shown graphically. When comparing the numerical results with results found in previous article,[11] it can be noted that the finite element method with increasing time becomes stable. In this regard, to obtain further propagation of the wave and its reflection in other domains becomes possible for two- and three-dimensional spaces also. This work provides a potential basis to consider two- and three-dimensional space for seismoacoustic equation[27-32] for future works to construct the neural networks and the deep learning models[33-35].

Acknowledgments

This work was supported by under the grant No. AP09058367 of the Committee of Science of the Ministry of Science and Higher Education of Kazakhstan (2021-2023).

Conflict of Interest

There is no conflict of interest.

Supporting Information

Not applicable.

References

[1] M. A. Biot, Theory of propagation of elastic waves in a fluid-saturated porous solid. I. low-frequency range, *The Journal of the Acoustical Society of America*, 1956, **28**, 168-178, doi: 10.1121/1.1908239.

[2] M. A. Biot, Theory of propagation of elastic waves in a fluid-saturated porous solid. II. higher frequency range, *The Journal of the Acoustical Society of America*, 1956, **28**, 179-191, doi: 10.1121/1.1908241.

[3] M. Biot, Generalized theory of acoustic propagation in porous dissipative media, *Journal of the Acoustical Society of America*, 1962, **34**, 1256-1264, doi: 10.1121/1.1918315.

[4] J. G. Berryman, Seismic wave attenuation in fluid-saturated porous media, *Pure and Applied Geophysics*

PAGEOPH, 1988, **128**, 423-432, doi: 10.1007/bf01772607.
[5] J. G. Berryman, Effective medium theories for multicomponent poroelastic composites, *Journal of Engineering Mechanics*, 2006, **132**, 519-531, doi: 10.1061/(asce)0733-9399(2006)132: 5(519).
[6] A. Mikeli´c, On the Effective Boundary Conditions Between Different Flow Regions, *Conference on Applied Mathematics and Computation Dubrovnik*, 1999, 9-18.
[7] R. Burridge, J. B. Keller, Poroelasticity equations derived from microstructure, *The Journal of the Acoustical Society of America*, 1981, **70**, 1140-1146, doi: 10.1121/1.386945.
[8] E. Sanchez-Palencia, Non-homogeneous media and vibration theory, *Lecture Notes in Physics*, 1980, **320**, 57-65, doi: 10.1007/3-540-10000-8.
[9] A. Meirmanov, Mathematical Models for Poroelastic Flows, Paris: Atlantis Press, 2014, doi: 10.2991/978-94-6239-015-7.
[10] A. Meirmanov, M. Nurtas, Mathematical models of seismics in composite media: elastic and poro-elastic components, *Journal of Differential Equations*, 2016, **2016**, 1-22.
[11] M. Nurtas, Zh. Baishemirov, S. Alpar, F. Tokmukhamedova, Numerical simulation of wave propagation in mixed porous media using finite element method, *Journal of Theoretical and Applied Information Technology*, 2021, **99**, 4163-4172.
[13] J. H. Mathews, K. D. Fink, Numerical methods using Matlab(Book), 4th edition, Prentice-Hall Inc., 2004, 430-436.
[14] A. Meirmanov, Double porosity models for liquid filtration in incompressible poroelastic media, *Mathematical Models and Methods in Applied Sciences*, 2010, **20**, 635-659, doi: 10.1142/s0218202510004374.
[15] S. Willard, Calculus and its applications, Prindle, Weber and Schmidt, Boston, 1976.
[16] L. V. Ovsyannikov, Lectures on basic gas dynamics, Institute of Computer Studies(Book), Moscow, Izhevsk, 2003.
[17] S. E. Buckley, M. C. Leverett, Mechanism of fluid displacement in sands, *Transactions of the AIME*, 1942, **146**, 107-116, doi: 10.2118/942107-g.
[18] V. Tournat, V. Pagneux, D. Lafarge, L. Jaouen, Multiple scattering of acoustic waves and porous absorbing media, *Physical Review E*, 2004, **70**, 026609, doi: 10.1103/physreve.70.026609.
[19] W. E. Ward, D. R. Kincaid, Numerical Mathematics and Computing, Cengage Learning, 2012.
[20] S. Mazumder, Numerical Methods for Partial Differential Equations, Academic Press, 2016.
[21] A. Meirmanov, M. Nurtas, Direct and inverse acoustic problems in porous media, Part I: formation of approximation solutions, Herald of Kazakh-British Technical University, 2015, 32.
[22] I. Malinouskaya, V. V. Mourzenko, J.-F. Thovert, P. M. Adler, Wave propagation through saturated porous media, *Physical Review E*, 2008, **77**, 066302, doi: 10.1103/physreve.77.066302.
[23] Larson M.G., Fredrik B. The Finite Element Method: Theory, Implementation, and Applications, 1 edition, Verlag Berlin Heidelberg: Springer, 2010.
[24] M. I. Protasov, G. V. Reshetova, V. A. Tcheverda, Fracture detection by Gaussian beam imaging of seismic data and image spectrum analysis, *Geophysical Prospecting*, 2016, **64**, 68-82, doi: 10.1111/1365-2478.12259.
[25] M. I. Protasov, V. A. Tcheverda, True amplitude elastic Gaussian beam imaging of multicomponent walkaway vertical seismic profiling data, *Geophysical Prospecting*, 2012, **60**, 1030-1042, doi: 10.1111/j.1365-2478.2012.01068.x.
[26] M. Mussatayev, M. Huang, M. Nurtas, A. Arynov, Improved calibration uncertainty assessment technique in coordinate metrology considering thermal influences, *Metrology and Measurement Systems*, 2021, **28**, 609-626, doi: 10.24425/Mms.2021.137699.
[27] D. Vishnevsky, V. Lisitsa, V. Tcheverda, G. Reshetova, Numerical study of the interface errors of finite-difference simulations of seismic waves, *Geophysics*, 2014, **79**, T219-T232, doi: 10.1190/geo2013-0299.1.
[28] A. Fichtner, Full Seismic Waveform Modelling and Inversion, Springer- Verlag Berlin Heidelberg Book, 2011, 113-140, doi: 10.1007/978-3-642-15807-0.
[29] M. Nurtas, Zh. Baishemirov, A. Ydyrys, A. Altaibek, 2-D Finite Element method using "eScript" for acoustic wave propagation, *ACM International Conference Proceeding Series*, 2020, **2020**, 3410774, doi: 10.1145/3410352.3410774.
[30] A. Sakabekov, Y. Auzhani, The solvability of mixed value problem for first and second approximations of one-dimensional nonlinear system of moment equations with macroscopic boundary conditions, *Journal of Nonlinear Mathematical Physics*, 2022, **29**, 124-148, doi:10.1007/s44198-021-00024-7.
[31] A. Sakabekov, Y. Auzhani, Boundary conditions for the onedimensional nonlinear nonstationary Boltzmann's moment system equations, *Journal of mathematical physics*, 2014, **55**, 123507, doi:10.1063/1.4902936.
[32] A. Sakabekov, Y. Auzhani approximation of the boundary value problem for 3-dimensional boltzmann's equation with maxwell's microscopic conditions, *Journal of mathematical physics*, 2019, **60**, 073508, doi:10.1063/1.5080797.
[33] M. Nurtas, Zh. Baishemirov, Zh. Zhanabekov, Applying Neural Network for predicting cardiovascular disase risk, *News of the National Academy of sciences of the Republic of Kazakhstan*, 2020, **4**, 28-34, doi: 10.32014/2020.2518-1726.62.
[34] M. Nurtas, Zh. Baishemirov, Zh. Zhanabekov, Convalutional Neural Networks as a method to solve estimation problem of acoustic wave propogation in poroelastic media, *News of the National Academy of sciences of the Republic of Kazakhstan*, 2020, **4**, 52-60, doi: 10.32014/2020.2518-1726.65.
[35] M. Nurtas, A.Ydyrys, A. Altaibek, Using of Machine Learning algorithm and Spectral method for simulation of Nonlinear Wave Equation, *ACM International Conference Proceeding Series*, 2020, **43**, 1-6, doi: 10.1145/3410352.3410778.